Journal of the Nigerian Association of Mathematical Physics
Volume 61 **(July – September** *2021 Issue*), pp77 – 90

IMPACT OF HEAT SOURCE, CHEMICAL REACTION AND SORET ON MHD PULSATILE FLOW OVER AN INCLINED POROUS PLATE WITH THERMAL RADIATION.

E. Omamoke[1], E. Amos[2] and I. Funakpo[1]

[1] Department of Mathematics, Bayelsa Medical University, Yenagoa, Bayelsa State, Nigeria.
[2] Department of Mathematics, Rivers State University, Port Harcourt, Nigeria.

Abstract

This study investigates the chemical reaction, thermal radiation, heat source and Soret effect on the pulsatile flow of a non-Newtonian, unsteady and incompressible MHD viscous fluid flowing past an inclined porous surface with the magnetic field acting on the porous surface of the plate. The dimensional governing equation was transformed to dimensionless form and then solved analytically using perturbation method. Conclusively, parameters such as chemical reaction, thermal radiation, heat source, inclined magnetic field and Soret number had an effect on the velocity profile, temperature profile, diffusion profile, heat transfer profile, skin friction profile and mass transfer profile with results discussed and graphically illustrated. Results showed that an increase in chemical reaction, Soret, angle of inclined plate to the vertical and suction causes an increase in the velocity flow while an increase in magnetic field, heat source and radiation reduces the velocity flow.

Keywords: Chemical Reaction, Thermal Radiation, Heat Source, Soret Effect, Inclined Plate, Permeability of Porous Plate, Magneto Hydrodynamic (MHD).

Nomenclature:

(x, y)	Cartesian coordinates (m)
α	Angle of inclined moving plate in the vertical direction
β	Angle of inclined moving plate in the horizontal direction
t	Time (s)
T_w	Temperature at the wall (K)
T_∞	Ambient temperature (K)
C_w	Concentration at the wall (mol/m^3)
C_∞	Ambient concentration (mol/m^3)
g	Acceleration due to gravity. (m/s^2)
V	Suction velocity (m/s)
u	Velocity in the x direction (m/s)
v	Velocity in the y direction (m/s)
B_0	Magnetic field (A/m)
K	Porosity parameter
C_p	Specific heat capacity $(m^2s^{-2}K^{-1})$
ρ	Density (kg/m^3)
∂_c	Electrical conductivity (A/m)
ϑ	Kinematic viscosity (m^2s^{-1})
δ'	Stefan-Boltzmann constant $(Wm^{-2}K^{-4})$
k	Coefficient of thermal conductivity $(Wm^{-1}K^{-1})$
K_T	Thermal diffusion ratio (m^2s^{-1})
H	Heat source parameter
So	Soret number
M	Magnetic parameter
G_T	Grashof temperature number
G_c	Grashof diffusion number
P_r	Prandtl number,
Sc	Schmidt number
R	Radiation parameter
q_r'	Radiative heat flux
Ec	Eckert number
A	Suction parameter
ε	Small positive constant
β_T	Coefficient of volume expansion due to temperature
β_C	Coefficient of volume expansion due to concentration
ω	Free stream frequency oscillation
Kr	Chemical reaction parameter
θ	Dimensionless temperature.
C	Dimensionless Concentration

Corresponding Author**:** Ekakitie O., Email: ekakitieomamoke@gmail.com, Tel: +2347037606266

1.0 Introduction

Engineering institutions and industries such as petrochemical, civil works, food production companies are mostly involved with fluids flow, heat and mass transfers during its operations. Examples of such include crude oil refining, building cooling systems, brewing production, paper production, food production, plastic production and others. Most often, the flow of heat and mass transfer considerably determines the quality of product produced. In [1], the influence of Dufour and Soret MHD flow in three dimension with chemical reaction and thermal radiation was studied. The nonlinear differential equations is transformed to ordinary differential equation and solved using homotopy analysis with the results showing that an increases in the magnetic field increases the velocity near the upper plate but reduced it near the lower plate, increase in radiation increase the temperature but increases in Prandtl number reduces the temperature, increase in the chemical reaction and Schmidt number increased the concentration profile, increase in Soret reduces the temperature but increases the concentration and increase in Dufour increases the temperature but reduces the concentration. Also, in [2] the effect of Soret, Dufour and Radiation on MHD unsteady flow past a porous plate that is inclined and enclosed in a medium that is porous with viscous dissipation was investigated. Numerical solution was used to solve the dimensionless governing equation using Crank-Nicolson finite difference method. Results showed that the increased Schmidt number and inclined angle caused a rapid decrease in the velocity, velocity increased mildly due to radiation and permeability increase, increase in magnetic field reduces the velocity, increase in Soret number increases the velocity and temperature but decreases the concentration while increase in Defour number decreases the velocity and increases the concentration initially before decreasing it. In [3], free convective MHD flow past a Porous Inclined Surface with effects of radiation and variable suction was investigated and studied. A study done in [4] showed the influence of radiation and viscous dissipation on free-convective MHD unsteady flow over an infinite vertical heated plate in a medium that is porous with time-dependent suction. In [5], the study on MHD thermos-solutal flow with Radiative Heat Transfer present over a Plate that Oscillates was investigated. In [6] MHD unsteady flow effect over a porous inclined plate that is embedded in a porous medium with the presence of viscous dissipation was studied. In [7], the Dufour and viscous dissipation effects on free convection MHD flow past a porous plate that is inclined and oscillating with ion-slip current and hall current was studied. In [8] the radiation, chemical reaction, and radiation influence on Nano MHD fluid flow over a flat permeable plate on porous medium was studied. In [9] the numerical study on the diffusion-thermo and diffusion effects on the two-phase boundary layer flow over a sheet stretching with suspended fluid particles and chemical reaction was investigated. In [10] the transfer of heat of thermal conductivity and variable viscosity effects on magnetic field that is inclined with dissipation in a non-Darcy medium was studied. The transfer of heat and mass on free convective MHD flow of fluid that is second grade through a porous medium over a vertical infinite plate was studied in [11]. In [12] he effect of porosity on MHD unsteady flow over a moving semi-infinite plate placed vertically with time dependent suction was studied. In [13], the effect of viscous dissipation and chemical reaction on free convection MHD flow over a moving semi –infinite vertical plate that is porous with radiation absorption was studied. In [14], a review on the effects of characteristics of heat transfer of Nano-fluids that is flowing under a turbulent and laminar flow regime was investigated. In [15] the unsteady free convective MHD heat and mass transfer on a boundary layer flow over a plate that is permeable and vertical with chemical reaction and thermal radiation was studied. The study of the effect of chemical reaction and inclined magnetic field on free convective flow over a porous plate that is semi finite and vertical through medium that is porous was done in [16]. In [17] the effect of chemical reaction and radiation on MHD transient free correction flow past a plate that is vertical through porous medium was studied. In [18], the effects of Defour and Soret on radiation Absorption fluid with exponential temperature and concentration present in a conducting field was also studied. The impact of heat source and chemical reaction on Free Convection MHD Flow past a porous surface that is inclined was studied in. In [20], the effect of radial magnetic field Soret of a free convective flow with slip in a viscous fluid that is reactive towards a porous cylinder that is vertical was studied. Also [21], the study of radiation and heat source effects on MHD free convection flow over an inclined porous plate in the presence of viscous dissipation was extensively studied with results discussed..

This research focuses on the chemical reaction, heat source and Soret effects on MHD pulsatile flow over an inclined porous plate with thermal radiation**.** Pertinent parameters such as Soret number, Magnetic field, Chemical reaction, Prandtl number, angle of the inclined plate in the vertical and horizontal direction, suction and radiation had an effect on velocity profile, temperature profile, concentration profile and heat transfer.

2. MATHEMATICAL FORMULATION

Unsteady free convective flow of an incompressible viscous Newtonian fluid that is chemically reactive, radiative and possess hydro magnetic fluid property over a semi-infinite plate inclined at an angle α in the vertical direction is considered. A magnetic field B_0 is applied in the vertical direction while the movement of the plate with uniform velocity V is in the horizontal direction. The temperature at the wall of the plate is greater than the temperature at the center i.e. $T_w > T_\infty$ and concentration at the wall of the plate is greater than the concentration at the center i.e. $C_w > C_\infty$. The Boussinesq approximation and the homogeneous chemical reaction of first and second order is assumed to be valid.

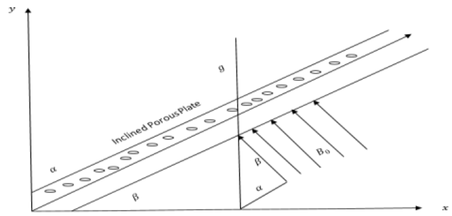

Figure 2.1 Geometry of the flow

Thus the flow equations are as follows.

$$\frac{\partial v'}{\partial y'} = 0 \quad (1)$$

$$\frac{\partial u'}{\partial t'} + v'\frac{\partial u'}{\partial y'} = -\frac{1}{\rho}\frac{\partial p'}{\partial x'} + \vartheta\frac{\partial^2 u'}{\partial y'} - \left[\delta_c B_0^2 cos^2\alpha + \frac{\vartheta}{k}\right]u' + gB_T(T' - T_\infty)\sin\beta + gB_C(C' - C_\infty)\sin\beta \quad (2)$$

$$\left(\frac{\rho C_p}{K_T}\right)\frac{\partial T'}{\partial t'} + v'\frac{\partial T'}{\partial y'} = \vartheta\frac{\partial^2 T'}{\partial y'^2} + \frac{Q_0}{K_T}(T' - T_\infty) - \frac{\partial q_r'}{\partial y'} \quad (3)$$

$$\frac{\partial C'}{\partial t'} + v'\frac{\partial C'}{\partial y'} = D\frac{\partial^2 C'}{\partial y'^2} - Kr'(C' - C_\infty) + Ho\frac{\partial^2 T'}{\partial y'^2} \quad (4)$$

The velocity, temperature and concentration profile in the above equations have the boundary conditions with the suction velocity term expressed as v' in [12]:

$$u' = U\ ;\ v' = -V(1 + \varepsilon Ae^{i\omega t});\ T_w{}' = T_w';\ C' = C_w'; \qquad at\ y = 0 \quad (6)$$

$$u = V(t) = V'(1 + \varepsilon Ae^{i\omega t});\ T' = T_\infty';\ C' = C_w' \qquad as\ y \to \infty \quad (7)$$

Consideration for approximation for the Rosseland diffusion term with the expression for the radiative heat flux q is looked at and given as in [13].

$$q_r' = -\frac{4\delta'}{3k'}\frac{\partial T'}{\partial y'} = -\frac{4\delta'}{3k'}\nabla T'$$

Where k' is the Roseland mean absorption coefficient and δ' is the Stefan – Boltzmann constant with the differences in the temperature of the flow is assumed to be small, such that the temperature linear function T' is expressed as

$T' = 4T_O^3 T - 3T_O'$ Meaning that

$$q_r' = -\frac{16\delta' T_O^3}{3k'}\frac{\partial T}{\partial y} \quad (8)$$

The non-dimensional quantities are introduced.

$$y = \frac{Vy'}{\vartheta};\ u = \frac{u'}{U}\ ;t = \frac{V'^2 t'}{\vartheta}\ ;\ \theta = \frac{T' - T_\infty}{T_W' - T_\infty}\ ; C = \frac{C' - C_\infty}{C_W' - C_\infty}; -\frac{dp}{dx} = Pe^{iwt} \quad (9)$$

$$M^2 = \frac{\vartheta\delta_c B_O^2}{\rho V^2}\ ;\ K = \frac{KV^2}{\vartheta^2}\ ;\ Re = \frac{Vd}{\vartheta}; G_T = \frac{g\vartheta B_T\theta(T_W{}' - T_\infty)}{UV^2}\ ;\ G_C = \frac{g\vartheta B_C C(C_W{}' - C_\infty)}{UV^2}\ ;\ \nu = \frac{\mu}{\rho};\ Pr = \frac{\mu C_p}{K_T};\ R^2 = \frac{16\delta' T_O^3}{3k'}\ ;\ E_C = \frac{U^2}{C_p(T_W' - T_\infty)}; Sc = \frac{\nu}{D};\ H = \frac{Q_0\nu}{\rho C_p V^2}; Kr = \frac{Kr'\vartheta^2}{DV^2}; So = \frac{Ho(T_W{}' - T_\infty)}{D(C_W{}' - C_\infty)}; \quad (10)$$

The momentum, energy and diffusion equation in dimensionless form is written as

$$\frac{\partial u}{\partial t} - (1 + \varepsilon Ae^{i\omega t})\frac{\partial u}{\partial y} = -\left(\frac{1}{Re}\right)\frac{\partial P}{\partial x} + \frac{\partial^2 u}{\partial y^2} - \left(M^2 cos^2\alpha + \frac{1}{K}\right)u + G_T\theta\sin\beta + G_C C\sin\beta \quad (11)$$

$$\frac{\partial\theta}{\partial t} - (1 + \varepsilon Ae^{i\omega t})\frac{\partial\theta}{\partial y} = \left(1 + \frac{R}{Pr}\right)\frac{\partial^2\theta}{\partial y^2} + H\theta \quad (12)$$

$$Sc\frac{\partial C}{\partial t} - Sc(1 + \varepsilon Ae^{i\omega t})\frac{\partial C}{\partial y} = \frac{\partial^2 C}{\partial y^2} - K_r C + So\frac{\partial^2\theta}{\partial y^2} \quad (13)$$

The corresponding boundary conditions in non-dimensional form are:

$$u = U = 1, \theta = 1, C = 1, \qquad at\ y = 0$$

$$u \to 0, \theta \to 0, C \to 0, \qquad at\ y \to \infty \quad (14)$$

3. METHOD OF SOLUTION

Equations (2) – (4) are nonlinear partial differential equations that is coupled and solved analytically which is later reduced to a set of ordinary differential equations with non-dimensional form gotten for the expressions of velocity (u), temperature (θ) and concentration (C) of the fluid:

$$u(y,t) = u_o(y) + \varepsilon e^{i\omega t}u_1 + 0(\varepsilon^2) \quad (15)$$

$$\theta(y,t) = \theta_o(y) + \varepsilon e^{i\omega t}\theta_1 + 0(\varepsilon^2) \quad (16)$$

$$C(y,t) = C_o(y) + \varepsilon e^{i\omega t} C_1 + 0(\varepsilon^2) \quad (17)$$

Substitute equation (15) to (17) into the set of equations (11), (12) and (13) and equate the non – harmonic and harmonic terms neglecting the terms of $0(\varepsilon^2)$, the set of ordinary differential equations are obtained with the required boundary condition.

$$u_0'' + u_0' - \left(M^2 cos^2\alpha + \frac{1}{K}\right) u_0 = -G_T\theta_0 \sin\beta - G_C C_0 \sin\beta \quad (18)$$

$$\left(1 - \frac{R}{Pr}\right)\theta_0'' + \theta_0' + H\theta_0 = 0 \quad (19)$$

$$C_0'' + ScC_0' - ScKrC_o = -So\theta_0'' \quad (20)$$

$$u_1'' + u_1' - \left(M^2 cos^2\alpha + \frac{1}{K} + i\omega\right) u_1 = -\frac{P}{Re} - Au_0' - G_T\theta_1 \sin\beta - G_C C_1 \sin\beta \quad (21)$$

$$\left(1 - \frac{R}{Pr}\right)\theta_1'' + P_r\theta_1' + [H - i\omega]\theta_1 = -A\theta_0' \quad (22)$$

$$C_1'' + ScC_1' - (Kr + Sci\omega)C_1 = -ScAC_0' - So\theta_1'' \quad (23)$$

Boundary conditions

$$u_0 = u; u_1 = 0;\ \theta_0 = 1;\ ,\theta_1 = 0;\ C_0 = 1;\ C_1 = 0 \qquad at\ y = 0 \quad (24)$$

$$u_0 \to 0; u_1 \to 0;\ \theta_0 \to 0;\ ,\theta_1 \to 0;\ C_0 \to 0;\ C_1 \to 0 \qquad as\ y \to \infty \quad (25)$$

Solving equations (18) – (23) with the boundary conditions (24) – (25) to obtain

$$u_0(y) = A_9e^{-m_5y} - A_{10}e^{-m_1y} - A_{11}e^{-m_3y} + A_{12}e^{-m_1y} \quad (26)$$

$$\theta_0(y) = e^{-m_1y} \quad (27)$$

$$C_0(y) = e^{-m_3y} - A_3e^{-m_1y} \quad (28)$$

$$u_1(y) = A_{13} + e^{-m_6y} - A_{14}e^{-m_5y} + A_{15}e^{-m_1y} - A_{16}e^{-m_2y} + A_{17}e^{-m_3y} - A_{18}e^{-m_4y} \quad (29)$$

$$\theta_1(y) = A_2(e^{-m_2y} + e^{-m_1y}) \quad (30)$$

$$C_1(y) = A_4e^{-m_4y} + A_5e^{-m_3y} - A_6e^{-m_1y} + A_7e^{-m_2y} - A_8e^{-m_1y} \quad (31)$$

Substitute equation (26) – (31) into equation (15) – (17), velocity, temperature and concentration profile will be expressed as,

$$u(y,t) = A_9e^{-m_5y} - A_{10}e^{-m_1y} - A_{11}e^{-m_3y} + A_{12}e^{-m_1y} + \varepsilon e^{i\omega t}(A_{13} + e^{-m_6y} - A_{14}e^{-m_5y} + A_{15}e^{-m_1y} - A_{16}e^{-m_2y} + A_{17}e^{-m_3y} - A_{18}e^{-m_4y}) \quad (32)$$

$$\theta(y,t) = e^{-m_1y} + \varepsilon e^{i\omega t}A_2(e^{-m_2y} + e^{-m_1y}) \quad (33)$$

$$C(y,t) = e^{-m_3y} - A_3e^{-m_1y} + \varepsilon e^{i\omega t}(A_4e^{-m_4y} + A_5e^{-m_3y} - A_6e^{-m_1y} + A_7e^{-m_2y} - A_8e^{-m_1y}) \quad (34)$$

The physical quantities of interest are the wall shear stress τ_w is given by

$$\tau_w = \mu\frac{\partial u^I}{\partial y^I} = \rho v_0^2 u^I(0)$$

The local skin friction factor

$$C_{fx} = \frac{\tau_w}{\rho v_0^2} = u^I(0) = -m_5A_9 + m_1A_{10} + m_3A_{11} - m_1A_{12} + \varepsilon e^{i\omega t}(-m_6 + m_5A_{14} - m_1A_{15} + m_2A_{16} - m_3A_{17} + m_4A_{18}) \quad (35)$$

The Local Surface heat Flux $q_r = \frac{-4\delta^I\partial T^I}{3k\partial y^I}$ where k is the effective thermal conductivity

Local Nusselt Number $N_{ux} = \frac{q_r}{T_w - T_\infty}$ where $q_r = \frac{-16\delta^I T_0^3 V_0^I (T_w - T_\infty)}{3k^I v}\frac{\partial\theta}{\partial y}$

Then $N_{ux} = \frac{-16\delta^I T_0^3 V_0^I}{3k^I v}\frac{\partial\theta}{\partial y}$ where $R_{ex} = \frac{-16\delta^I T_0^3 V_0^I}{3k^I v}$

$$\frac{N_{ux}}{R_{ex}} = \frac{\partial\theta}{\partial y} = \theta^I(0) = -m_1 + \varepsilon e^{i\omega t}A_2(m_1 - m_2) \quad (36)$$

The local surface mass flux is given by

$$\frac{Sh_x}{R_{ex}} = -\frac{\partial C}{\partial y} = C^I(0) = -m_3 - m_1A_3 + \varepsilon e^{i\omega t}(-m_4A_4 - m_3A_5 - m_2A_7 + m_1(A_6 + A_8) \quad (37)$$

4. RESULTS AND DISCUSSIONS

Different parameters had resulting effects on the velocity, temperature, concentration, skin friction, heat transfer and mass flux rate which is discussed. In Figure 4.1, it is observed that an increase in the chemical reaction results to an increase in the velocity of the fluid flow while the increase in the Soret number causes the velocity of the fluid flow to increase in Figure 4.2. In Figure 4.3, an increase in the Schmidt number causes the velocity of the fluid flow to increase. Heat source increase in Figure 4.4 reduces the velocity of the fluid flow while increase in the magnetic field reduces the velocity of the fluid flow in Figure 4.5 as a result of Lorentz force which introduces resistance to the fluid flow. In Figure 4.6, the increase in the thermal radiation reduces the velocity of the fluid flow while increase in the Grashof temperature number increases the velocity of the fluid flow in Figure 4.7. Increase in the Grashof diffusion number reduces the velocity of the fluid flow

in Figure 4.8 while increase in the angle of the inclined plate in the vertical direction increases the velocity of the fluid flow in Figure 4.9. Increase in the angle of the inclined plate in the horizontal direction causes an increase in the velocity of the fluid flow in Figure 4.10 while an increase in suction increases the velocity of the fluid flow in Figure 4.11. In Figure 4.12, an increase in the Prandtl number reduces the velocity of the fluid flow while in Figure 4.13, an increase in heat source increases the temperature of the fluid. In Figure 4.14, an increase in radiation reduces the temperature of the fluid and in Figure 4.15 the increase in suction increases the temperature of the fluid. In Figure 4.16, an increase in Prandtl number increases the temperature of the fluid while in Figure 4.17 an increase in chemical reaction reduces the concentration of the fluid. In Figure 4.18, the increase in the Soret number causes an increase in the concentration profile but the observation in Figure 4.19 shows that, an increase in Schmidt number increases the concentration near the plate but reduces far from the plate. It is observed that in Figure 4.20, an increase in heat source increases the concentration of the fluid, an increase in the radiation increases the concentration of the fluid in Figure 4.21, an increase in suction decreases the concentration of the fluid in Figure 4.22, while an increase in the Prandtl number increases the concentration in Figure 4.23. The increase in chemical reaction and Soret number increases the skin friction in Figure 4.24 and Figure 4.25, increase in heat source decreases the skin friction profile in Figure 4.26, an increase in the magnetic field increases the skin friction in Figure 4.27 while an increase in the radiation parameter resulted to a decrease in the skin friction profile in Figure 4.28. It is also observed that an increase in the Grashof diffusion number and Grashof temperature number increases the skin friction in Figure 4.29, Figure 4.30, while an increase in the angle of the inclined plate in the vertical direction reduces the skin friction profile in Figure 4.31. In Figure 4.32, an increase in the suction results to an increase in the skin friction profile but an increase in heat source and the thermal radiation initially increases the heat transfer but then it reduces afterward in Figure 4.33 and Figure 4.34. In Figure 4.35 and 4.36, an increase in the both suction and Prandtl number increases the heat transfer profile. Finally, an increase in the chemical reaction and suction in Figure 4.37 and Figure 4.41 reduces the mass transfer profile, but an increase in Soret number, heat source, thermal radiation and Prandtl number increases the mass transfer profile in
Figure 4.38, 4.39, 4.40 and 4.42.

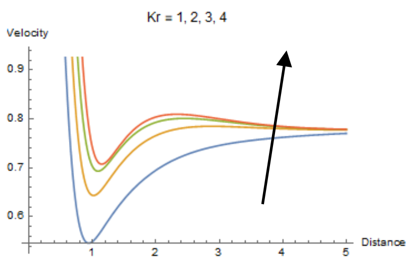

Figure 4.1 **Velocity Profile with Variation of Chemical Reaction Kr**
$M = 2, So = 2, P_r = 0.71, S_c = 0.22, G_r = 5, G_c = 10, K = 2, R = 0.1, H = 0.1, A = 1, P = 2, Re = 0.5, \alpha = 30, \beta = 30, \omega = 1, t = 1, \varepsilon = 1$

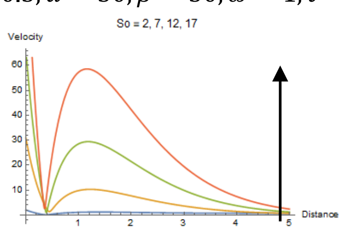

Figure 4.2 **Velocity Profile with Variation of Soret Number So**
$M = 2, P_r = 0.71, S_c = 0.22, G_r = 5, G_c = 10, \mathrm{Kr} = 1, K = 2, R = 0.1, H = 0.1, A = 1, P = 2, Re = 0.5, \alpha = 30, \beta = 30, \omega = 1, t = 1, \varepsilon = 1$

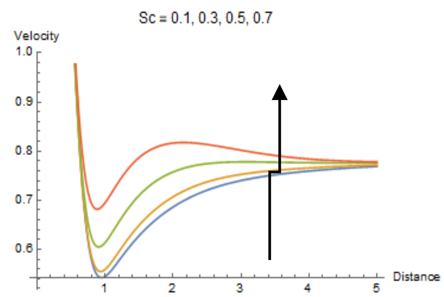

Figure 4.3 **Velocity Profile with Variation of Schmidt Number Sc**
$M = 2, So = 2, P_r = 0.71, G_r = 5, G_c = 10, \mathrm{Kr} = 1, K = 2, R = 0.1, H = 0.1, A = 1, P = 2, Re = 0.5, \alpha = 30, \beta = 30, \omega = 1, t = 1, \varepsilon = 1$

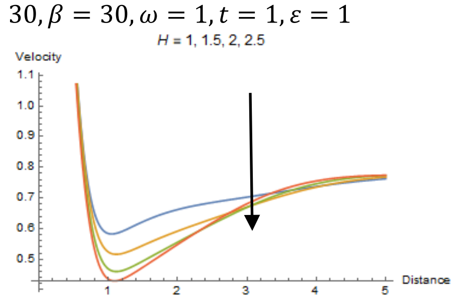

Figure 4.4 **Velocity Profile with Variation of Heat Source H**
$M = 2, So = 2, P_r = 0.71, S_c = 0.22, G_r = 5, G_c = 10, \mathrm{Kr} = 1, K = 2, R = 0.1, A = 1, P = 2, Re = 0.5, \alpha = 30, \beta = 30, \omega = 1, t = 1, \varepsilon = 1$

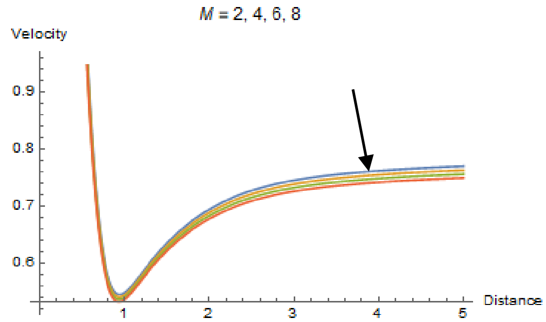

Figure 4.5 **Velocity Profile with Variation of Magnetic Field Parameter *M***
$So = 2, P_r = 0.71, S_c = 0.22, G_r = 5, G_c = 10, \mathrm{Kr} = 1, K = 2, R = 0.1, H = 0.1, A = 1, P = 2, Re = 0.5, \alpha = 30, \beta = 30, \omega = 1, t = 1, \varepsilon = 1$

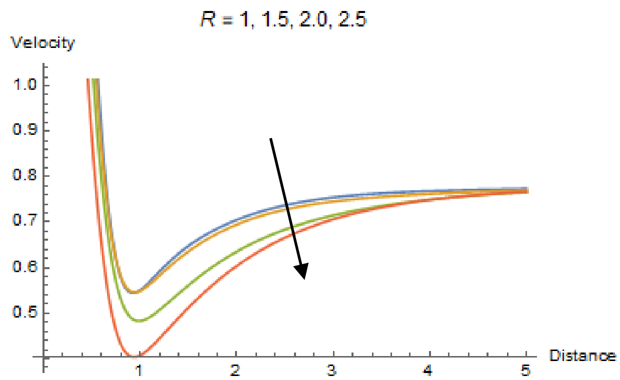

Figure 4.6 **Velocity Profile with Variation of Radiation Parameter R**
$M = 2, So = 2, P_r = 0.71, S_c = 0.22, G_r = 5, G_c = 10, \mathrm{Kr} = 1, K = 2, H = 0.1, A = 1, P = 2, Re = 0.5, \alpha = 30, \beta = 30, \omega = 1, t = 1, \varepsilon = 1$

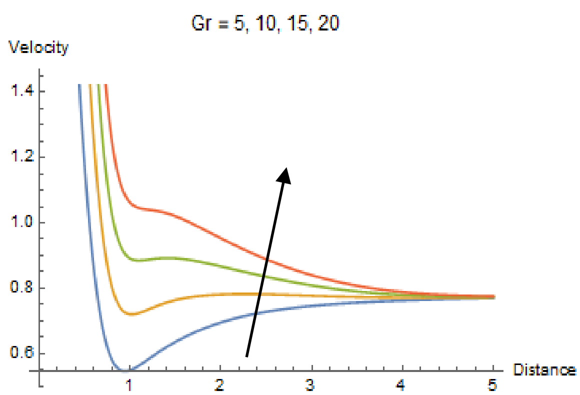

Figure 4.7 **Velocity Profile with Variation of Grashof temperature Number Gr**
$M = 2, So = 2, P_r = 0.71, S_c = 0.22, G_c = 10, \mathrm{Kr} = 1, K = 2, R = 0.1, H = 0.1, A = 1, P = 2, Re = 0.5, \alpha = 30, \beta = 30, \omega = 1, t = 1, \varepsilon = 1$

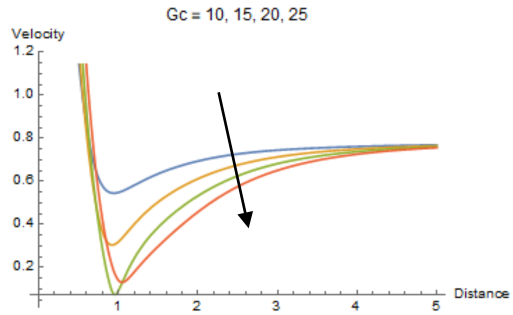

Figure 4.8 **Velocity Profile with Variation of Grashof Diffusion Number Gc**
$M = 2, So = 2, P_r = 0.71, S_c = 0.22, G_r = 5, \mathrm{Kr} = 1, K = 2, R = 0.1, H = 0.1, A = 1, P = 2, Re = 0.5, \alpha = 30, \beta = 30, \omega = 1, t = 1, \varepsilon = 1$

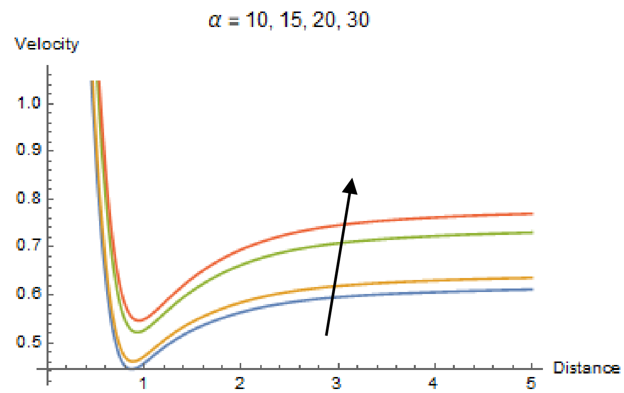

Figure 4.9 **Velocity Profile with Variation of angle of inclined plate to the vertical** α
$M = 2, So = 2, P_r = 0.71, S_c = 0.22, G_r = 5, G_c = 10, \mathrm{Kr} = 1, K = 2, R = 0.1, H = 0.1, A = 1, P = 2, Re = 0.5, \beta = 30, \omega = 1, t = 1, \varepsilon = 1$

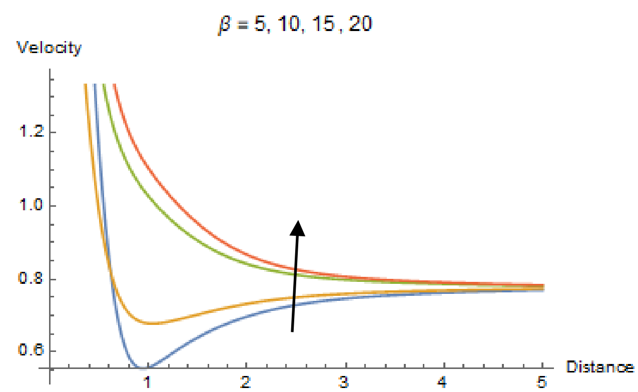

Figure 4.10 **Velocity Profile with Variation of angle of inclined plate to the horizontal** β
$M = 2, So = 2, P_r = 0.71, S_c = 0.22, G_r = 5, G_c = 10, \mathrm{Kr} = 1, K = 2, R = 0.1, H = 0.1, A = 1, P = 2, Re = 0.5, \alpha = 30, \omega = 1, t = 1, \varepsilon = 1$

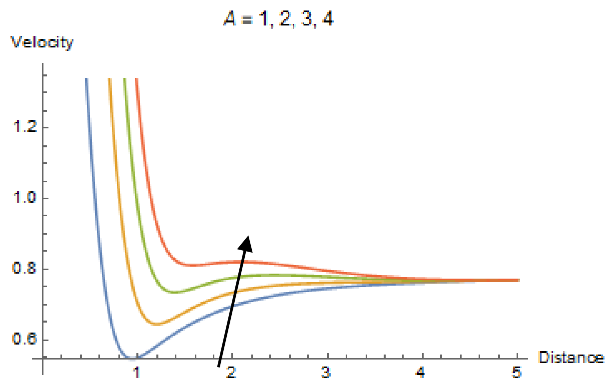

Figure 4.11 **Velocity Profile with Variation of Suction Parameter A**
$M = 2, So = 2, P_r = 0.71, S_c = 0.22, G_r = 5, G_c = 10, \mathrm{Kr} = 1, K = 2, R = 0.1, H = 0.1, P = 2, Re = 0.5, \alpha = 30, \beta = 30, \omega = 1, t = 1, \varepsilon = 1$

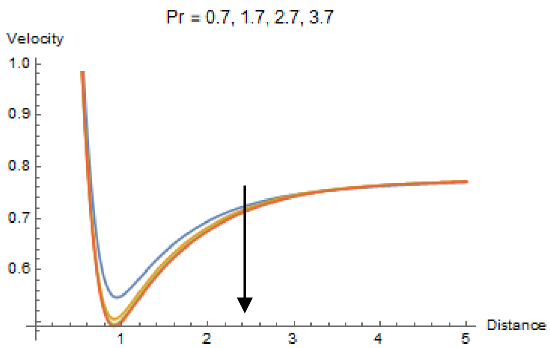

Figure 4.12 **Velocity Profile with Variation of Prandtl Number Pr**
$M = 2, So = 2, S_c = 0.22, G_r = 5, G_c = 10, \mathrm{Kr} = 1, K = 2, R = 0.1, H = 0.1, A = 1, P = 2, Re = 0.5, \alpha = 30, \beta = 30, \omega = 1, t = 1, \varepsilon = 1$

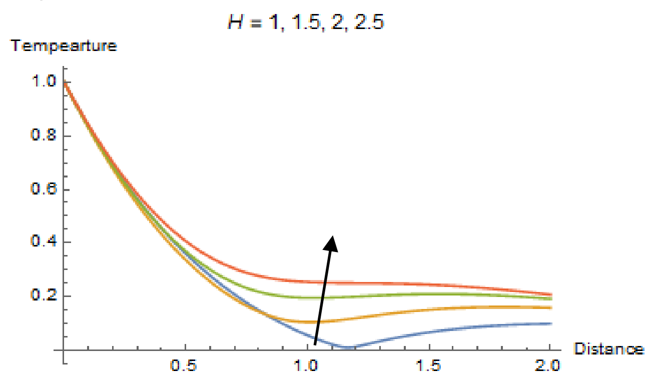

Figure 4.13 **Temperature Profile with Variation of Heat Source H**
$P_r = 0.71, R = 0.1, A = 1, \omega = 1, t = 1, \varepsilon = 1$

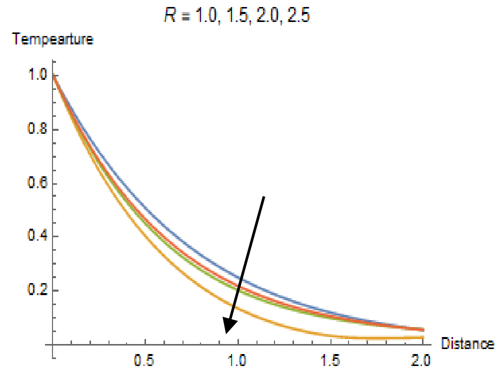

Figure 4.14 **Temperature Profile with Variation of Radiation R**
$P_r = 0.71, H = 0.1, A = 1, \omega = 1, t = 1, \varepsilon = 1$

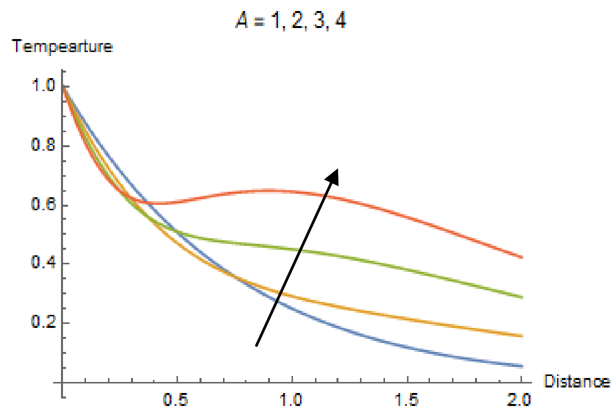

Figure 4.15 **Temperature Profile with Variation of Suction A**
$P_r = 0.71, R = 0.1, H = 0.1, \omega = 1, t = 1, \varepsilon = 1$

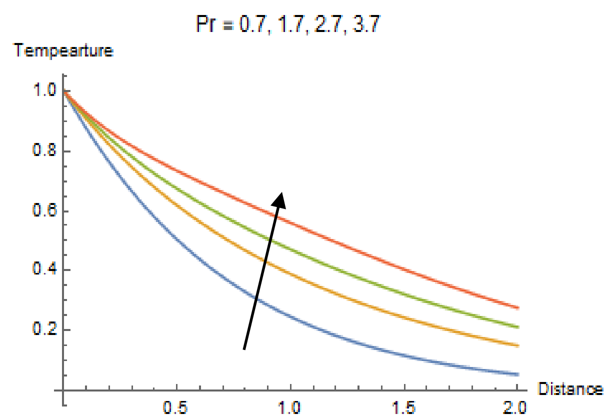

Figure 4.16 **Temperature Profile with Variation of Radiation R**
$R = 0.1, H = 0.1, A = 1, \omega = 1, t = 1, \varepsilon = 1$

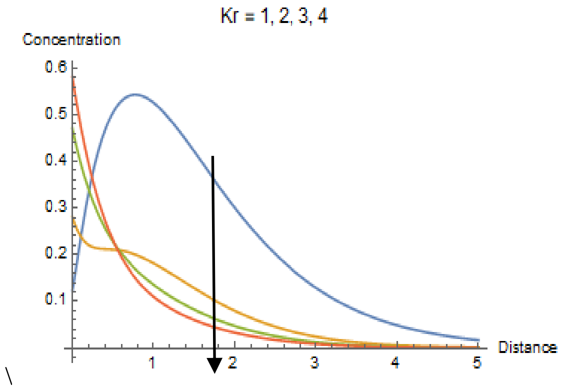

\

Figure 4.17 **Concentration Profile with Variation of Chemical Reaction Kr**
$So = 2, P_r = 0.71, S_c = 0.22, \mathrm{Kr} = 1, K = 2, R = 0.1, H = 0.1, A = 1, \omega = 1, t = 1, \varepsilon = 1$

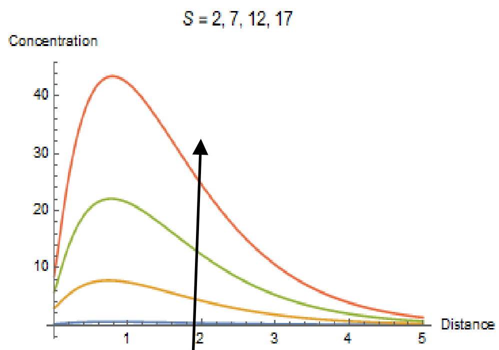

Figure 4.18 **Concentration Profile with Variation of Soret Number So**
$So = 2, P_r = 0.71, S_c = 0.22, \mathrm{Kr} = 1, K = 2, R = 0.1, H = 0.1, A = 1, \omega = 1, t = 1, \varepsilon = 1$

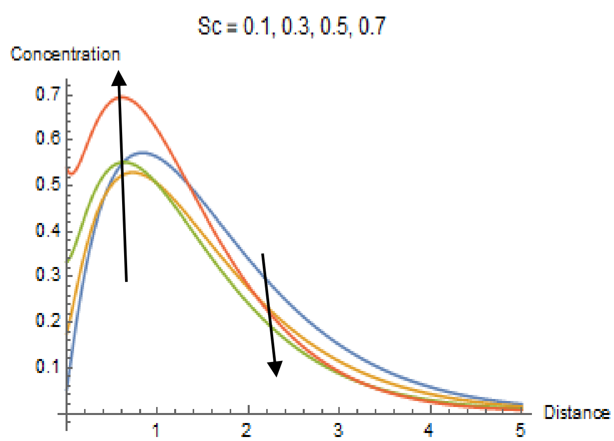

Figure 4.19 **Concentration Profile with Variation of Schmidt Number Sc**
$So = 2, P_r = 0.71, S_c = 0.22, \mathrm{Kr} = 1, K = 2, R = 0.1, H = 0.1, A = 1, \omega = 1, t = 1, \varepsilon = 1$

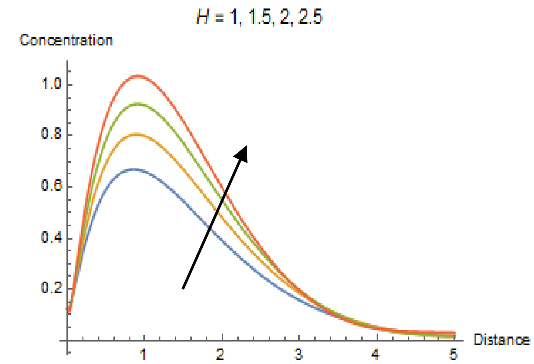

Figure 4.20 **Concentration Profile with Variation of Heat Source H**
$So = 2, P_r = 0.71, S_c = 0.22, \mathrm{Kr} = 1, K = 2, R = 0.1, H = 0.1, A = 1, \omega = 1, t = 1, \varepsilon = 1$

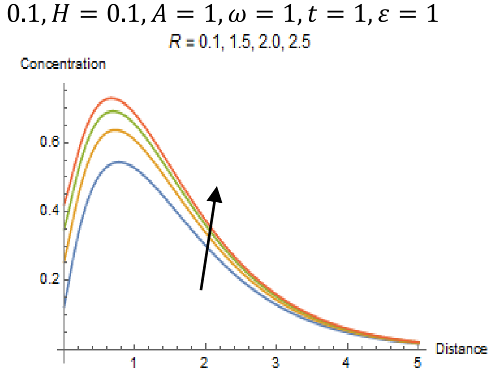

Figure 4.21 **Concentration Profile with Variation of Radiation R**
$So = 2, P_r = 0.71, S_c = 0.22, \mathrm{Kr} = 1, K = 2, R = 0.1, H = 0.1, A = 1, \omega = 1, t = 1, \varepsilon = 1$

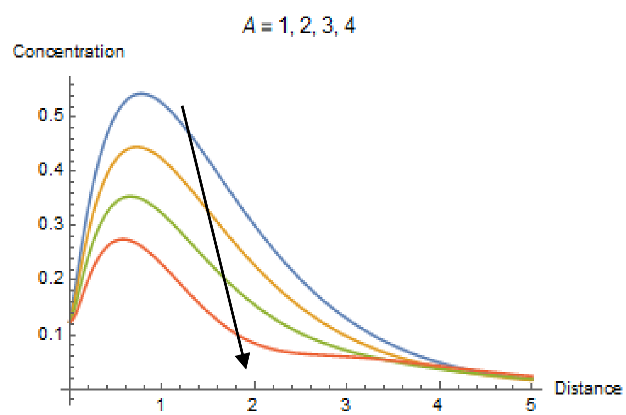

Figure 4.22 **Concentration Profile with Variation of Suction A**
$So = 2, P_r = 0.71, S_c = 0.22, \mathrm{Kr} = 1, K = 2, R = 0.1, H = 0.1, A = 1, \omega = 1, t = 1, \varepsilon = 1$

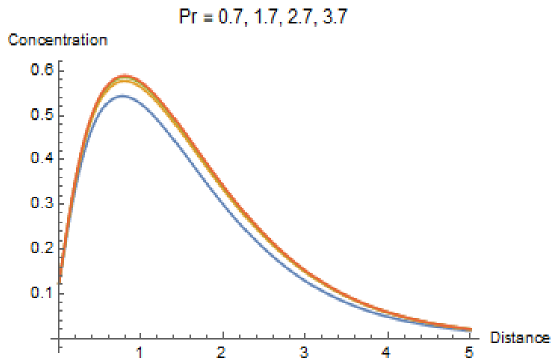

Figure 4.23 **Concentration Profile with Variation of Prandtl Number Pr**
$So = 2, P_r = 0.71, S_c = 0.22, \mathrm{Kr} = 1, K = 2, R = 0.1, H = 0.1, A = 1, \omega = 1, t = 1, \varepsilon = 1$

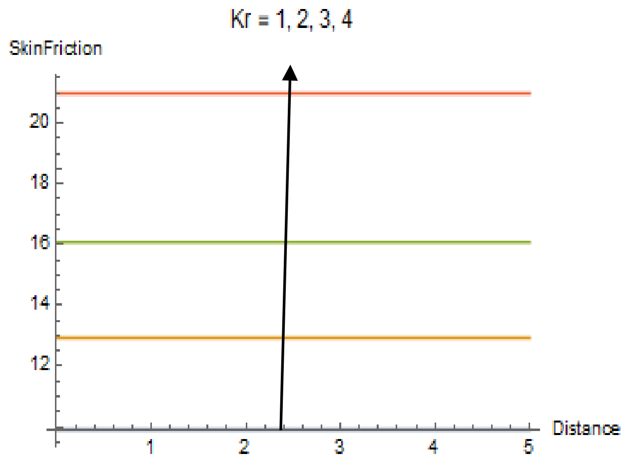

Figure 4.24 **Skin Friction Profile with Variation of Chemical Reaction Kr**
$M = 2, So = 2, P_r = 0.71, S_c = 0.22, G_r = 5, G_c = 10, K = 2, R = 0.1, H = 0.1, A = 1, P = 2, Re = 0.5, \alpha = 30, \beta = 30, \omega = 1, t = 1, \varepsilon = 1$

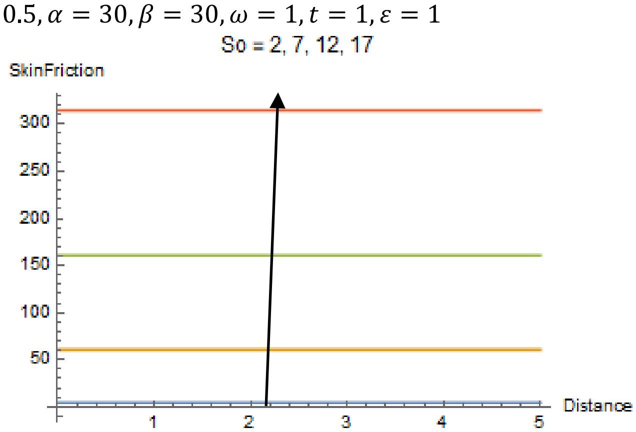

Figure 4.25 **Skin Friction Profile with Variation of Soret Number So**
$M = 2, P_r = 0.71, S_c = 0.22, G_r = 5, G_c = 10, \mathrm{Kr} = 1, K = 2, R = 0.1, H = 0.1, A = 1, P = 2, Re = 0.5, \alpha = 30, \beta = 30, \omega = 1, t = 1, \varepsilon = 1$

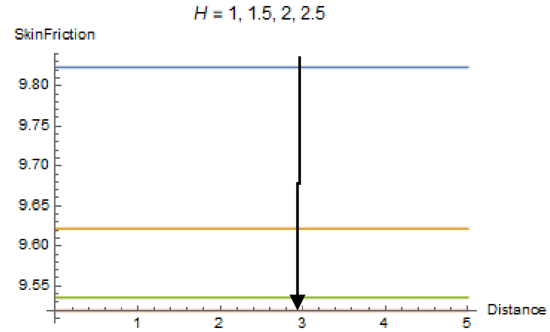

Figure 4.26 **Skin Friction Profile with Variation of Heat Source H**
$M = 2, So = 2, P_r = 0.71, S_c = 0.22, G_r = 5, G_c = 10, \mathrm{Kr} = 1, K = 2, R = 0.1, A = 1, P = 2, Re = 0.5, \alpha = 30, \beta = 30, \omega = 1, t = 1, \varepsilon = 1$

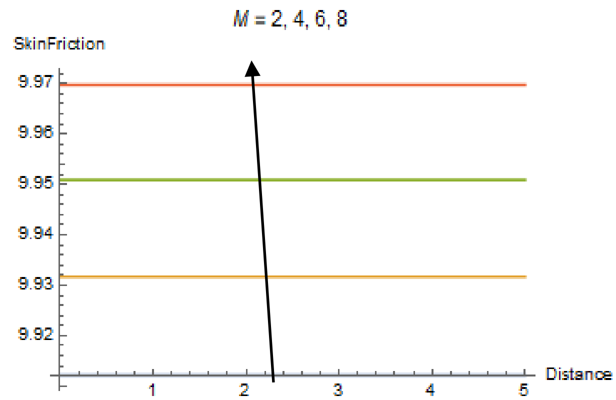

Figure 4.27 **Skin Friction Profile with Variation of Magnetic Field Parameter *M***
$So = 2, P_r = 0.71, S_c = 0.22, G_r = 5, G_c = 10, \mathrm{Kr} = 1, K = 2, R = 0.1, H = 0.1, A = 1, P = 2, Re = 0.5, \alpha = 30, \beta = 30, \omega = 1, t = 1, \varepsilon = 1$

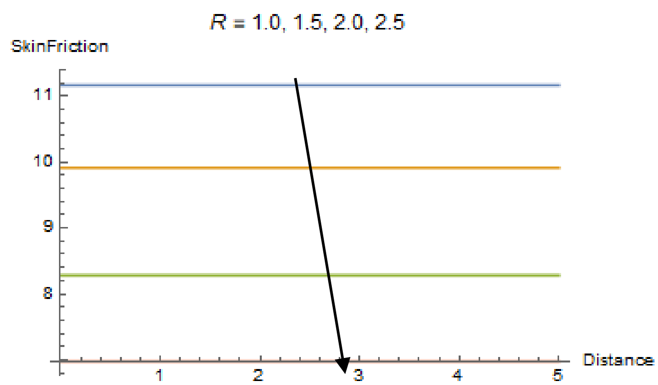

Figure 4.28 **Skin Friction Profile with Variation of Radiation Parameter R**
$M = 2, So = 2, P_r = 0.71, S_c = 0.22, G_r = 5, G_c = 10, \mathrm{Kr} = 1, K = 2, H = 0.1, A = 1, P = 2, Re = 0.5, \alpha = 30, \beta = 30, \omega = 1, t = 1, \varepsilon = 1$

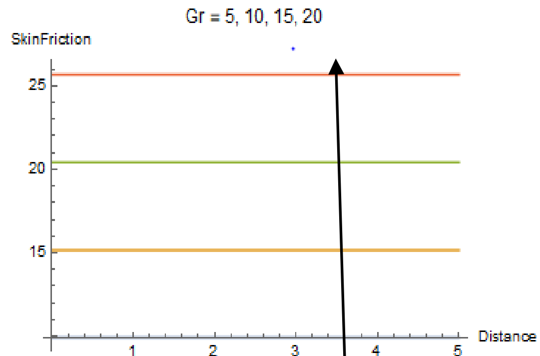

Figure 4.29 **Skin Friction with Variation of Grashof temperature Number Gr**
$M = 2, So = 2, P_r = 0.71, S_c = 0.22, G_c = 10, \mathrm{Kr} = 1, K = 2, R = 0.1, H = 0.1, A = 1, P = 2, Re = 0.5, \alpha = 30, \beta = 30, \omega = 1, t = 1, \varepsilon = 1$

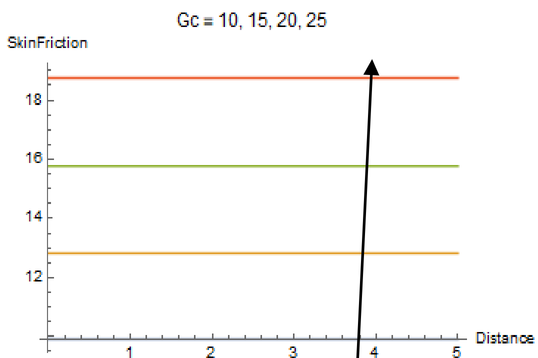

Figure 4.30 **Skin Friction Profile with Variation of Grashof Diffusion Number Gc**
$M = 2, So = 2, P_r = 0.71, S_c = 0.22, G_r = 5, \mathrm{Kr} = 1, K = 2, R = 0.1, H = 0.1, A = 1, P = 2, Re = 0.5, \alpha = 30, \beta = 30, \omega = 1, t = 1, \varepsilon = 1$

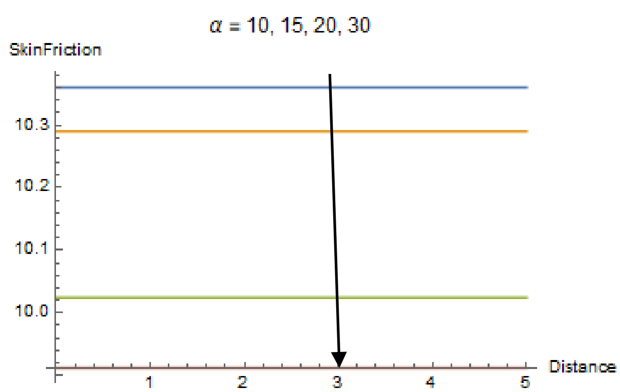

Figure 4.31 **Skin Friction Profile with Variation of angle of inclined plate to the vertical** α
$M = 2, So = 2, P_r = 0.71, S_c = 0.22, G_r = 5, G_c = 10, \mathrm{Kr} = 1, K = 2, R = 0.1, H = 0.1, A = 1, P = 2, Re = 0.5, \beta = 30, \omega = 1, t = 1, \varepsilon = 1$

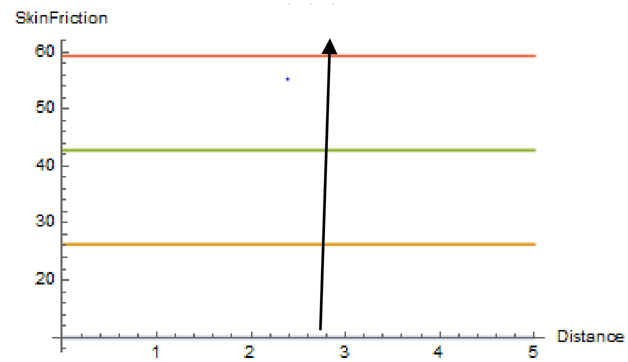

Figure 4.32 **Skin Friction with Variation of Suction Parameter A**
$M = 2, So = 2, P_r = 0.71, S_c = 0.22, G_r = 5, G_c = 10, \mathrm{Kr} = 1, K = 2, R = 0.1, H = 0.1, P = 2, Re = 0.5, \alpha = 30, \beta = 30, \omega = 1, t = 1, \varepsilon = 1$

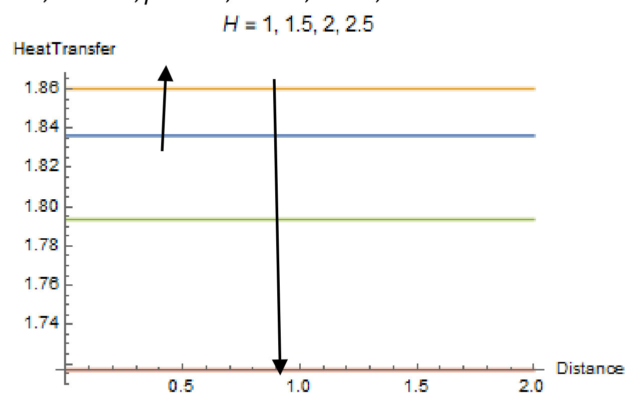

Figure 4.33 **Heat Transfer Profile with Variation of Heat Source H**
$P_r = 0.71, R = 0.1, A = 1, \omega = 1, t = 1, \varepsilon = 1$

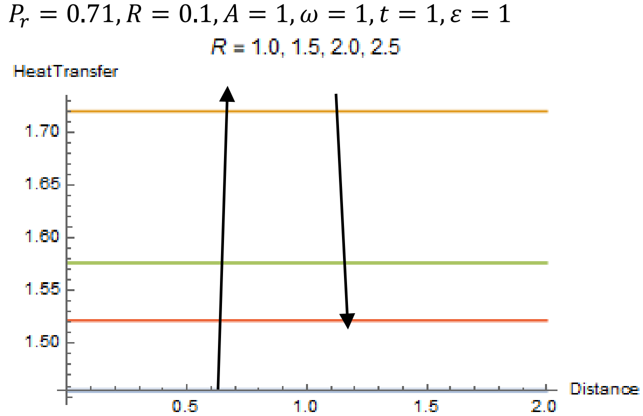

Figure 4.34 **Heat Transfer Profile with Variation of Radiation R**
$P_r = 0.71, H = 0.1, A = 1, \omega = 1, t = 1, \varepsilon = 1$

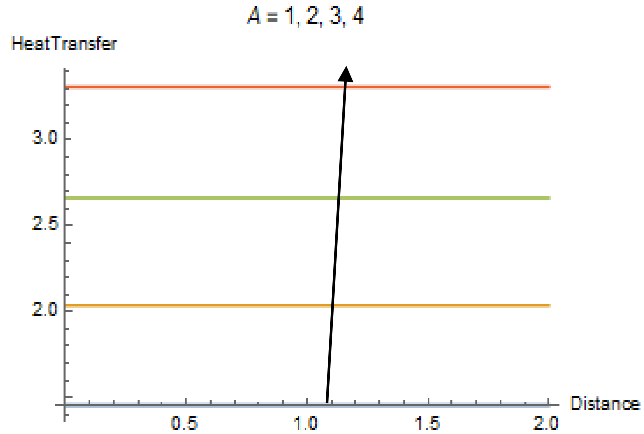

Figure 4.35 **Heat Transfer Profile with Variation of Suction A**
$P_r = 0.71, R = 0.1, H = 0.1, \omega = 1, t = 1, \varepsilon = 1$

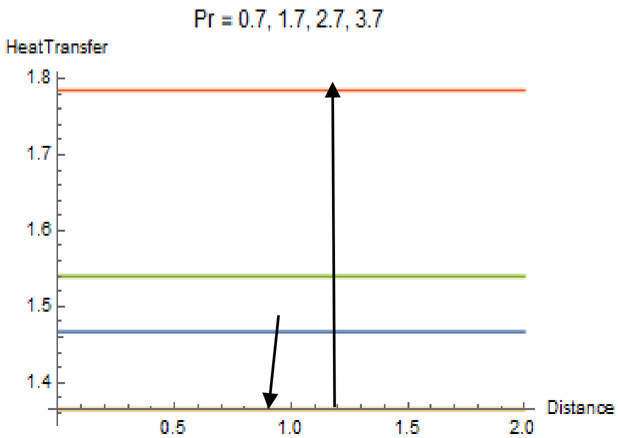

Figure 4.36 **Heat Transfer Profile with Variation of Radiation R**
$R = 0.1, H = 0.1, A = 1, \omega = 1, t = 1, \varepsilon = 1$

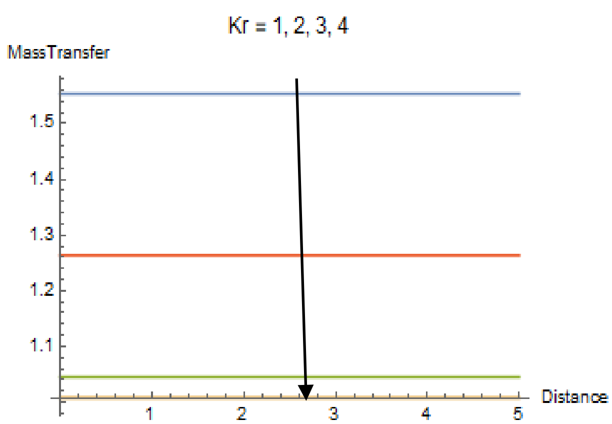

Figure 4.37 **Mass Transfer Profile with Variation of Chemical Reaction Kr**
$So = 2, P_r = 0.71, S_c = 0.22, \mathrm{Kr} = 1, K = 2, R = 0.1, H = 0.1, A = 1, \omega = 1, t = 1, \varepsilon = 1$

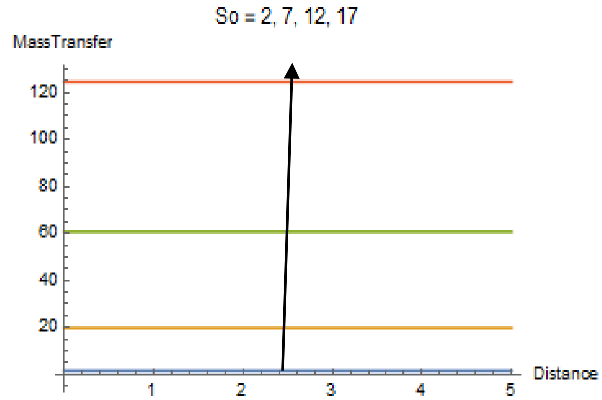

Figure 4.38 **Mass Transfer Profile with Variation of Soret Number So**
$So = 2, P_r = 0.71, S_c = 0.22, \mathrm{Kr} = 1, K = 2, R = 0.1, H = 0.1, A = 1, \omega = 1, t = 1, \varepsilon = 1$

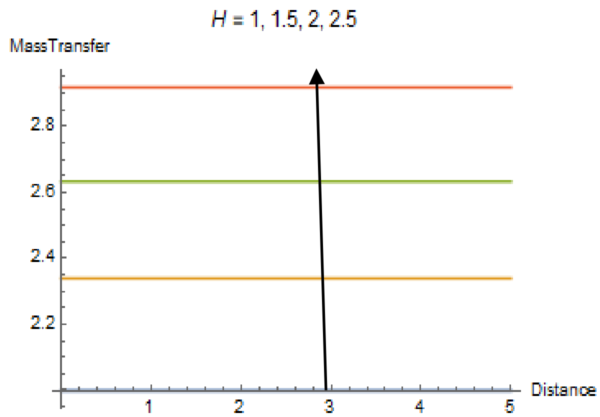

Figure 4.39 **Mass Transfer Profile with Variation of Heat Source H**
$So = 2, P_r = 0.71, S_c = 0.22, \mathrm{Kr} = 1, K = 2, R = 0.1, H = 0.1, A = 1, \omega = 1, t = 1, \varepsilon = 1$

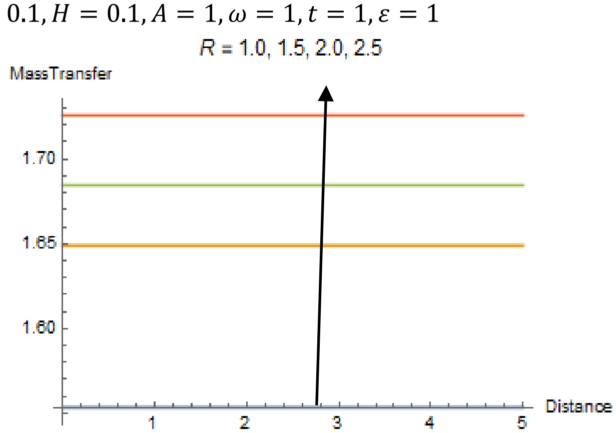

Figure 4.40 **Mass Transfer Profile with Variation of Radiation R**
$So = 2, P_r = 0.71, S_c = 0.22, \mathrm{Kr} = 1, K = 2, R = 0.1, H = 0.1, A = 1, \omega = 1, t = 1, \varepsilon = 1$

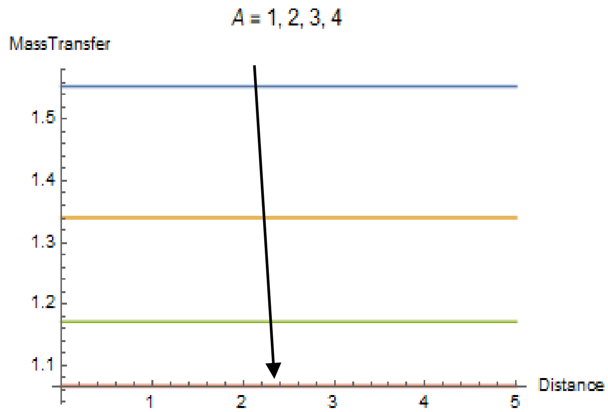

Figure 4.41 **Mass Transfer Profile with Variation of Suction A**
$So = 2, P_r = 0.71, S_c = 0.22, \mathrm{Kr} = 1, K = 2, R = 0.1, H = 0.1, A = 1, \omega = 1, t = 1, \varepsilon = 1$

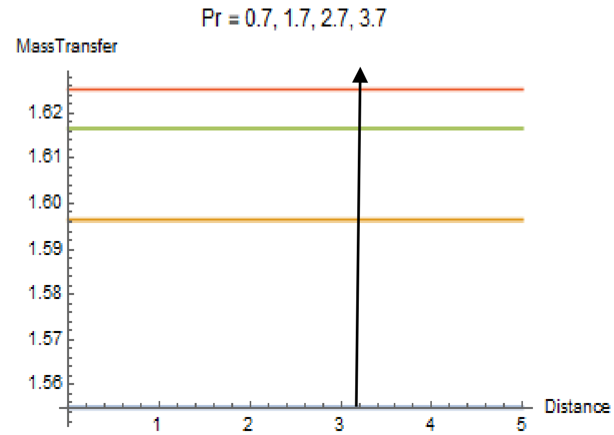

Figure 4.42 **Mass Transfer Profile with Variation of Prandtl Number Pr**
$So = 2, P_r = 0.71, S_c = 0.22, \mathrm{Kr} = 1, K = 2, R = 0.1, H = 0.1, A = 1, \omega = 1, t = 1, \varepsilon = 1$

5. CONCLUSION

Radiation, Heat source, Viscous dissipation and Soret effects on MHD free convection flow over an inclined plate that is porous are summarized as follows,

I. An increase in chemical reaction causes an increase in velocity, skin friction and a decrease in chemical reaction
II. An increase in magnetic field reduces the velocity flow and increases the skin friction.
III. An increase in heat source reduces the velocity flow and skin friction but causes an increase in the temperature, concentration and mass transfer.
IV. An increases in radiation reduces the velocity flow, temperature and skin friction but causes an increase in the concentration.
V. An increase in Soret increases the velocity flow, concentration, skin friction and mass transfer.
VI. An increase in the angle of inclined plate to the vertical increases the velocity flow and reduces the skin friction while in increase in the angle of the inclined plate to the horizontal increases the velocity
VII. Increase in suction increases the velocity, temperature and skin friction but reduces the concentration and mass transfer.

Areas of applicability of the results discussed in this study include crude oil refining, building cooling systems, brewing production, paper production, food production, plastic production and others.

APPENDIX

$\mathrm{m1} = \frac{1}{2}\left(1 + \sqrt{1 - 4H\left(\frac{1-R}{\mathrm{Pr}}\right)}\right)$; $\mathrm{m2} = \frac{1}{2}\left(1 + \sqrt{1 - 4(H - i\omega)}\right)$;

$\mathrm{m3} = \frac{1}{2}(\mathrm{Sc} + \sqrt{(\mathrm{Sc})^2 + 4\mathrm{Kr}})$; $\mathrm{m4} = \frac{1}{2}(\mathrm{Sc} + \sqrt{(\mathrm{Sc})^2 + 4(\mathrm{Kr} + \mathrm{Sc}i\omega)})$;

$\mathrm{m5} = \frac{1}{2}(1 + \sqrt{1 + 4(M\mathrm{Cos}[\alpha]^2 + \frac{1}{k}})$); $\mathrm{m6} = \frac{1}{2}(1 + \sqrt{1 + 4(i\omega + M\mathrm{Cos}[\alpha]^2 + \frac{1}{k}})$);

$\mathrm{A2} = \frac{A}{(1-\frac{R}{\mathrm{Pr}})\mathrm{m1}^2 + \mathrm{m1} - (H - i\omega)}$; $\mathrm{A3} = \frac{So\mathrm{m1}^2}{\mathrm{m1}^2 - \mathrm{Scm1} + \mathrm{Kr}}$; $\mathrm{A4} = -\mathrm{A5} + \mathrm{A6} - \mathrm{A7} + \mathrm{A8}$;

$\mathrm{A5} = \frac{A\mathrm{Scm3}}{\mathrm{m3}^2 - \mathrm{m3} - (\mathrm{Kr} + \mathrm{Sc}i\omega)}$; $\mathrm{A6} = \frac{\mathrm{A3Scm1}}{\mathrm{m1}^2 - \mathrm{m1} - (\mathrm{Kr} + \mathrm{Sc}i\omega)}$; $\mathrm{A7} = \frac{So\mathrm{A3m2}^2}{\mathrm{m2}^2 - \mathrm{m2} - (\mathrm{Kr} + \mathrm{Sc}i\omega)}$;

$\mathrm{A8} = \frac{So\mathrm{A2m1}^2}{\mathrm{m1}^2 - \mathrm{m1} - (\mathrm{Kr} + \mathrm{Sc}i\omega)}$; $\mathrm{A9} = \mathrm{A10} + \mathrm{A11} - \mathrm{A12}$; $\mathrm{A10} = \frac{\mathrm{GrSin}[\beta]}{\mathrm{m1}^2 - \mathrm{m1} - (M\mathrm{Cos}[\alpha]^2 + \frac{1}{k})}$;

$\mathrm{A11} = \frac{\mathrm{GcSin}[\beta]}{\mathrm{m3}^2 - \mathrm{m3} - \left(M\mathrm{Cos}[\alpha]^2 + \frac{1}{k}\right)}$; $\mathrm{A12} = \frac{\mathrm{A3GcSin}[\beta]}{\mathrm{m1}^2 + \mathrm{m1} - \left(M\mathrm{Cos}[\alpha]^2 + \frac{1}{k}\right)}$;

$\mathrm{A14} = \frac{A\mathrm{m5A9}}{\mathrm{m5}^2 - \mathrm{m5} - (i\omega + M\mathrm{Cos}[\alpha]^2 + \frac{1}{k})}$; $\mathrm{A13} = \frac{P}{Re(i\omega + M\mathrm{Cos}[\alpha]^2 + \frac{1}{k})}$;

$\mathrm{A15} = \frac{A(\mathrm{m5A12} - \mathrm{m5A10}) + \mathrm{A2GrSin}[\beta] + \mathrm{GcSin}[\beta](\mathrm{A6} + \mathrm{A8})}{\mathrm{m1}^2 - \mathrm{m1} - (i\omega + M\mathrm{Cos}[\alpha]^2 + \frac{1}{k})}$; $\mathrm{A16} = \frac{\mathrm{A2GrSin}[\beta] + \mathrm{A7GcSin}[\beta]}{\mathrm{m2}^2 - \mathrm{m2} - (i\omega + M\mathrm{Cos}[\alpha]^2 + \frac{1}{k})}$;

$\mathrm{A17} = \frac{A\mathrm{m3A11} - \mathrm{A5GcSin}[\beta]}{\mathrm{m3}^2 - \mathrm{m3} - (i\omega + M\mathrm{Cos}[\alpha]^2 + \frac{1}{k})}$; $\mathrm{A18} = \frac{\mathrm{A4GcSin}[\beta]}{\mathrm{m4}^2 - \mathrm{m4} - (i\omega + M\mathrm{Cos}[\alpha]^2 + \frac{1}{k})}$;

References

[1] Sharma, K. & Bhaskar, K. (2019). Influence of Soret and Dufour on three dimensional MHD flow considering thermal radiation and chemical reaction. International Journal of Applied Computational Mathematics, 6(1), DOI: 10.1007/s40819.

[2] Panday, N. & Shurkla, A. K, (2014). Soret-Dufour and radiation effects on unsteady MHD flow over an inclined porous plate embedded in porous medium with viscous dissipation. International Journal of advances in applied mathematics and mechanics, 2(1), 107-119, ISSN: 2347-2529, www.ijaamm.

[3] Amos, E. and Omamoke. E., (2018). MHD Free Convetive Flow over an Inclined Porous Surface with Variable Suction and Radiation Effects. International Journal of Applied Science and Mathematical Theory, ISSN 2489-009X, Vol. 4, No. 3.

[4] Israel-Cookey, C., Ogulu A. and V.B. Omubo-Pepple. (2002). Influence of viscous dissipation and radiation on unsteady MHD free-convection flow past an infinite heated vertical plate in a porous medium with time-dependent suction, International Journal of Heat and Mass Transfer 46 (2003) 2305–2311 Received 1 August 2002; received in revised form 9.

[5] Mebine, P. (2007). Thermosolutal MHD Flow with Radiative Heat Transfer past an Oscillating Plate. Advances in Theoretical and Applied Mathematics, 2, 3, pp 217-231.

[6] Pandya, N. Shukla, A. K., and Sorel-Du, Effect on unsteady MHD flow over an inclined porous plate embedded in porous medium with viscous dissipation, International Journal of Applied Mathematics and Mechanics 2[1] [2014] 107-119, ISSN;2347-2529.

[7]. Raja Kumer, K. V. B., Balamunigen K. S., Ramana Murthy Ch.V. & Rarjaneth N. (2018). Viscous dissipation and Dufour effects on MHD free convection flow through an oscillatory inclined porous plate with hall and ion-slip current. International Journal of Engineering and Technology, 7[4.5], pp. 410-415.

[8] Ramman Reddy, J. V., Suyunamama, V., Sandeep, N. & Sulochana, C. (2016). Influence of chemical reaction, radiation and rotation on MHD Nano fluid flow past a permeable flat plate on porous medium. Journal of the Nigerian Mathematical Society, 35, pp. 48-65.

[9] Krupalakshimi, K. L., Gireesha, B. J.,Gorla Rama, S. R. & Mahanthesh, B. (2016). Effect of diffusion-thermo and diffusion on the two-phase boundary layer flow past a stretching sheet with fluid particles suspension and chemical reaction: A numerical study. Journal of Mathematical Society, 35, pp. 66 - 81.

[10] Salawu, S. O. & Dada, M. S. (2016). Heat transfer of variable viscosity and thermal conductivity effects on inclined magnetic field with dissipation in a non-Darcy medium, Journal of the Nigerian Mathematical Society, 35, pp. 93-106.

[11] Basu, D.O., Venkataswarlu, S. & Reddy, E. K. (2017). Heat and mass transfer on MHD free convective flow of second grade fluid through porous medium over an infinite vertical plate. IOP conference series, Materials Science and Engineering. 225, 012267, DOI:10.1088/1757-899x/225/1/0122.

[12] Ram, P., Kumar, A. & Singh, H. (2013). Effect of porosity on unsteady MHD flow past a semi-infinite moving vertical plate with time dependent suction. Indian journal of pure and applied physics, volume 51, pp. 461-470.

[13] Rajakumar, K. V. B, Balamurugan, K. S., Murthy, Ch. V. & Reddy, U. M. (2017). Chemical reaction and viscous dissipation effect on MHD free convection flow past a semi –infinite moving vertical porous plate with radiation absorption. Global Journal of Pure and Applied Mathematics, 13(12), pp. 8297-8322, ISSN 0973-1768.

[14] Kumar, P. & Padey, K. M. (2017). Effects on heat transfer characteristics of Nano fluids flowing under laminar and turbulent flow regime. A review, I0P Conference. Series: Science and Engineering, 225, 012168, DOI:10.1088/1757-899x/225/1/012168.

[15] Venkateswarlu, M. & Polarapu, P. (2015). Unsteady MHD free convective heat and mass transfer on a boundary layer flow past a vertical permeable plate with thermal radiation and chemical reaction. Procedia Engineering 127, 791-799.

[16] Sugnamma, V., Serndeep, N., Mohan-Krishina, P. & Ramana, B., Inclined magnetic field and chemical reaction effect on flow over a semi finite vertical porous plate through porous medium, communications in applied sciences, 1(1), 1-24, ISSN2201-7372, 2015.

[17] Sandeep, N., Reddy, A. B. V. & Sugunamma, V. (2012). Effect of radiation and chemical reaction on transient MHD free correction flow over a vertical plate through porous media chemical and process engineering research, volume2, 2012, www.liste.org.

[18] Harinath, Reddy, S., Raju, M. C. & Reddy, Keshava, E., (2016). Soret and Defour Effects on Radiation Absorption Fluid in the Presence of Exponentially Varying Temperature and Concentration in a Conducting Field, Special Topics and Reviews in Porous Media-An International Journal 7(2):115-129.

[19] Ekakitie, Omamoke & Emeka, Amos, (2020). The Impact of Chemical Reaction and Heat Source on MHD Free Convection Flow over an Inclined Porous Surface. International Journal of Scientific and Research Publication, Volume 10, Issue 5, ISSN: 2250-3153, DOI: 10.29322/IJSRP.10.05.2020.P10103.

[20] Ojemeri, G., Onwabuya, I. O. & Abdusalam, S. (2020). Effect of Soret and Radial Magnetic Field of a Free Convective Slip Flow in a Viscous Reactive Fluid towards a Vertical Porous Cylinder. Continental Journal of Applied Sciences, 14 (1): 25-45 DOI: 10.5281, ISSN: 1597-9928.

[21] Omamoke, E., Amos, E., & Funakpo, I. (2020). Radiation and Heat Source Effect on MHD Free Convection Flow over an Inclined Porous Plate in the Presence of Viscous Dissipation. American Journal of Applied Mathematics, 8(4), 190 – 206, ISSN: 2330-0043.